

Measurement of time-dependent CP asymmetries in $B^0 \rightarrow D^{(*)\pm} \pi^\mp$ and $B^0 \rightarrow D^\pm \rho^\mp$ decays

B. Aubert,¹ R. Barate,¹ D. Boutigny,¹ F. Couderc,¹ Y. Karyotakis,¹ J. P. Lees,¹ V. Poireau,¹ V. Tisserand,¹
A. Zghiche,¹ E. Grauges,² A. Palano,³ M. Pappagallo,³ J. C. Chen,⁴ N. D. Qi,⁴ G. Rong,⁴ P. Wang,⁴ Y. S. Zhu,⁴
G. Eigen,⁵ I. Ofte,⁵ B. Stugu,⁵ G. S. Abrams,⁶ M. Battaglia,⁶ D. S. Best,⁶ D. N. Brown,⁶ J. Button-Shafer,⁶
R. N. Cahn,⁶ E. Charles,⁶ C. T. Day,⁶ M. S. Gill,⁶ A. V. Gritsan,^{6,*} Y. Groysman,⁶ R. G. Jacobsen,⁶ J. A. Kadyk,⁶
L. T. Kerth,⁶ Yu. G. Kolomensky,⁶ G. Kukartsev,⁶ G. Lynch,⁶ L. M. Mir,⁶ P. J. Oddone,⁶ T. J. Orimoto,⁶
M. Pripstein,⁶ N. A. Roe,⁶ M. T. Ronan,⁶ W. A. Wenzel,⁶ M. Barrett,⁷ K. E. Ford,⁷ T. J. Harrison,⁷ A. J. Hart,⁷
C. M. Hawkes,⁷ S. E. Morgan,⁷ A. T. Watson,⁷ M. Fritsch,⁸ K. Goetzen,⁸ T. Held,⁸ H. Koch,⁸ B. Lewandowski,⁸
M. Pelizaeus,⁸ K. Peters,⁸ T. Schroeder,⁸ M. Steinke,⁸ J. T. Boyd,⁹ J. P. Burke,⁹ W. N. Cottingham,⁹ D. Walker,⁹
T. Cuhadar-Donszelmann,¹⁰ B. G. Fulsom,¹⁰ C. Hearty,¹⁰ N. S. Knecht,¹⁰ T. S. Mattison,¹⁰ J. A. McKenna,¹⁰
A. Khan,¹¹ P. Kyberd,¹¹ M. Saleem,¹¹ L. Teodorescu,¹¹ V. E. Blinov,¹² A. D. Bukin,¹² A. Buzykaev,¹²
V. P. Druzhinin,¹² V. B. Golubev,¹² A. P. Onuchin,¹² S. I. Serednyakov,¹² Yu. I. Skovpen,¹² E. P. Solodov,¹² K. Yu
Todyshev,¹² M. Bondioli,¹³ M. Bruinsma,¹³ M. Chao,¹³ S. Curry,¹³ I. Eschrich,¹³ D. Kirkby,¹³ A. J. Lankford,¹³
P. Lund,¹³ M. Mandelkern,¹³ R. K. Mommsen,¹³ W. Roethel,¹³ D. P. Stoker,¹³ S. Abachi,¹⁴ C. Buchanan,¹⁴
S. D. Foulkes,¹⁵ J. W. Gary,¹⁵ O. Long,¹⁵ B. C. Shen,¹⁵ K. Wang,¹⁵ L. Zhang,¹⁵ D. del Re,¹⁶ H. K. Hadavand,¹⁶
E. J. Hill,¹⁶ H. P. Paar,¹⁶ S. Rahatlou,¹⁶ V. Sharma,¹⁶ J. W. Berryhill,¹⁷ C. Campagnari,¹⁷ A. Cunha,¹⁷
B. Dahmes,¹⁷ T. M. Hong,¹⁷ J. D. Richman,¹⁷ T. W. Beck,¹⁸ A. M. Eisner,¹⁸ C. J. Flacco,¹⁸ C. A. Heusch,¹⁸
J. Kroseberg,¹⁸ W. S. Lockman,¹⁸ G. Nesom,¹⁸ T. Schalk,¹⁸ B. A. Schumm,¹⁸ A. Seiden,¹⁸ P. Spradlin,¹⁸
D. C. Williams,¹⁸ M. G. Wilson,¹⁸ J. Albert,¹⁹ E. Chen,¹⁹ G. P. Dubois-Felsmann,¹⁹ A. Dvoretzskii,¹⁹ D. G. Hitlin,¹⁹
I. Narsky,¹⁹ T. Piatenko,¹⁹ F. C. Porter,¹⁹ A. Ryd,¹⁹ A. Samuel,¹⁹ R. Andreassen,²⁰ G. Mancinelli,²⁰
B. T. Meadows,²⁰ M. D. Sokoloff,²⁰ F. Blanc,²¹ P. C. Bloom,²¹ S. Chen,²¹ W. T. Ford,²¹ J. F. Hirschauer,²¹
A. Kreisel,²¹ U. Nauenberg,²¹ A. Olivas,²¹ W. O. Ruddick,²¹ J. G. Smith,²¹ K. A. Ulmer,²¹ S. R. Wagner,²¹
J. Zhang,²¹ A. Chen,²² E. A. Eckhart,²² A. Soffer,²² W. H. Toki,²² R. J. Wilson,²² F. Winklmeier,²² Q. Zeng,²²
D. D. Altenburg,²³ E. Feltresi,²³ A. Hauke,²³ H. Jasper,²³ B. Spaan,²³ T. Brandt,²⁴ V. Klose,²⁴ H. M. Lacker,²⁴
R. Nogowski,²⁴ A. Petzold,²⁴ J. Schubert,²⁴ K. R. Schubert,²⁴ R. Schwierz,²⁴ J. E. Sundermann,²⁴ A. Volk,²⁴
D. Bernard,²⁵ G. R. Bonneaud,²⁵ P. Grenier,^{25,†} E. Latour,²⁵ Ch. Thiebaux,²⁵ M. Verderi,²⁵ D. J. Bard,²⁶
P. J. Clark,²⁶ W. Gradl,²⁶ F. Muheim,²⁶ S. Playfer,²⁶ Y. Xie,²⁶ M. Andreotti,²⁷ D. Bettoni,²⁷ C. Bozzi,²⁷
R. Calabrese,²⁷ G. Cibinetto,²⁷ E. Luppi,²⁷ M. Negrini,²⁷ L. Piemontese,²⁷ F. Anulli,²⁸ R. Baldini-Ferrolì,²⁸
A. Calcaterra,²⁸ R. de Sangro,²⁸ G. Finocchiaro,²⁸ S. Pacetti,²⁸ P. Patteri,²⁸ I. M. Peruzzi,^{28,‡} M. Piccolo,²⁸
A. Zallo,²⁸ A. Buzzo,²⁹ R. Capra,²⁹ R. Contri,²⁹ M. Lo Vetere,²⁹ M. M. Macri,²⁹ M. R. Monge,²⁹ S. Passaggio,²⁹
C. Patrignani,²⁹ E. Robutti,²⁹ A. Santroni,²⁹ S. Tosi,²⁹ G. Brandenburg,³⁰ K. S. Chaisanguanthum,³⁰ M. Morii,³⁰
J. Wu,³⁰ R. S. Dubitzky,³¹ J. Marks,³¹ S. Schenk,³¹ U. Uwer,³¹ W. Bhimji,³² D. A. Bowerman,³² P. D. Dauncey,³²
U. Egede,³² R. L. Flack,³² J. R. Gaillard,³² J. A. Nash,³² M. B. Nikolich,³² W. Panduro Vazquez,³² X. Chai,³³
M. J. Charles,³³ W. F. Mader,³³ U. Mallik,³³ V. Ziegler,³³ J. Cochran,³⁴ H. B. Crawley,³⁴ L. Dong,³⁴ V. Eyges,³⁴
W. T. Meyer,³⁴ S. Prell,³⁴ E. I. Rosenberg,³⁴ A. E. Rubin,³⁴ G. Schott,³⁵ N. Arnaud,³⁶ M. Davier,³⁶
G. Grosdidier,³⁶ A. Höcker,³⁶ F. Le Diberder,³⁶ V. Lepeltier,³⁶ A. M. Lutz,³⁶ A. Oyanguren,³⁶ T. C. Petersen,³⁶
S. Pruvot,³⁶ S. Rodier,³⁶ P. Roudeau,³⁶ M. H. Schune,³⁶ A. Stocchi,³⁶ W. F. Wang,³⁶ G. Wormser,³⁶ C. H. Cheng,³⁷
D. J. Lange,³⁷ D. M. Wright,³⁷ C. A. Chavez,³⁸ I. J. Forster,³⁸ J. R. Fry,³⁸ E. Gabathuler,³⁸ R. Gamet,³⁸
K. A. George,³⁸ D. E. Hutchcroft,³⁸ D. J. Payne,³⁸ K. C. Schofield,³⁸ C. Touramanis,³⁸ A. J. Bevan,³⁹
F. Di Lodovico,³⁹ W. Menges,³⁹ R. Sacco,³⁹ C. L. Brown,⁴⁰ G. Cowan,⁴⁰ H. U. Flaecher,⁴⁰ D. A. Hopkins,⁴⁰
P. S. Jackson,⁴⁰ T. R. McMahon,⁴⁰ S. Ricciardi,⁴⁰ F. Salvatore,⁴⁰ D. N. Brown,⁴¹ C. L. Davis,⁴¹ J. Allison,⁴²
N. R. Barlow,⁴² R. J. Barlow,⁴² Y. M. Chia,⁴² C. L. Edgar,⁴² M. P. Kelly,⁴² G. D. Lafferty,⁴² M. T. Naisbit,⁴²
J. C. Williams,⁴² J. I. Yi,⁴² C. Chen,⁴³ W. D. Hulsbergen,⁴³ A. Jawahery,⁴³ D. Kovalskyi,⁴³ C. K. Lae,⁴³
D. A. Roberts,⁴³ G. Simi,⁴³ G. Blaylock,⁴⁴ C. Dallapiccola,⁴⁴ S. S. Hertzbach,⁴⁴ X. Li,⁴⁴ T. B. Moore,⁴⁴ S. Saremi,⁴⁴

H. Staengle,⁴⁴ S. Y. Willocq,⁴⁴ R. Cowan,⁴⁵ K. Koeneke,⁴⁵ G. Sciolla,⁴⁵ S. J. Sekula,⁴⁵ M. Spitznagel,⁴⁵ F. Taylor,⁴⁵ R. K. Yamamoto,⁴⁵ H. Kim,⁴⁶ P. M. Patel,⁴⁶ C. T. Potter,⁴⁶ S. H. Robertson,⁴⁶ A. Lazzaro,⁴⁷ V. Lombardo,⁴⁷ F. Palombo,⁴⁷ J. M. Bauer,⁴⁸ L. Cremaldi,⁴⁸ V. Eschenburg,⁴⁸ R. Godang,⁴⁸ R. Kroeger,⁴⁸ J. Reidy,⁴⁸ D. A. Sanders,⁴⁸ D. J. Summers,⁴⁸ H. W. Zhao,⁴⁸ S. Brunet,⁴⁹ D. Côté,⁴⁹ M. Simard,⁴⁹ P. Taras,⁴⁹ F. B. Viaud,⁴⁹ H. Nicholson,⁵⁰ N. Cavallo,^{51,§} G. De Nardo,⁵¹ F. Fabozzi,^{51,§} C. Gatto,⁵¹ L. Lista,⁵¹ D. Monorchio,⁵¹ D. Piccolo,⁵¹ C. Sciacca,⁵¹ M. Baak,⁵² H. Bulten,⁵² G. Raven,⁵² H. L. Snoek,⁵² C. P. Jessop,⁵³ J. M. LoSecco,⁵³ T. Allmendinger,⁵⁴ G. Benelli,⁵⁴ K. K. Gan,⁵⁴ K. Honscheid,⁵⁴ D. Hufnagel,⁵⁴ P. D. Jackson,⁵⁴ H. Kagan,⁵⁴ R. Kass,⁵⁴ T. Pulliam,⁵⁴ A. M. Rahimi,⁵⁴ R. Ter-Antonyan,⁵⁴ Q. K. Wong,⁵⁴ N. L. Blount,⁵⁵ J. Brau,⁵⁵ R. Frey,⁵⁵ O. Igonkina,⁵⁵ M. Lu,⁵⁵ R. Rahmat,⁵⁵ N. B. Sinev,⁵⁵ D. Strom,⁵⁵ J. Strube,⁵⁵ E. Torrence,⁵⁵ F. Galeazzi,⁵⁶ A. Gaz,⁵⁶ M. Margoni,⁵⁶ M. Morandin,⁵⁶ A. Pompili,⁵⁶ M. Posocco,⁵⁶ M. Rotondo,⁵⁶ F. Simonetto,⁵⁶ R. Stroili,⁵⁶ C. Voci,⁵⁶ M. Benayoun,⁵⁷ J. Chauveau,⁵⁷ P. David,⁵⁷ L. Del Buono,⁵⁷ Ch. de la Vaissière,⁵⁷ O. Hamon,⁵⁷ B. L. Hartfiel,⁵⁷ M. J. J. John,⁵⁷ Ph. Leruste,⁵⁷ J. Malcès,⁵⁷ J. Ocariz,⁵⁷ L. Roos,⁵⁷ G. Therin,⁵⁷ P. K. Behera,⁵⁸ L. Gladney,⁵⁸ J. Panetta,⁵⁸ M. Biasini,⁵⁹ R. Covarelli,⁵⁹ M. Pioppi,⁵⁹ C. Angelini,⁶⁰ G. Batignani,⁶⁰ S. Bettarini,⁶⁰ F. Bucci,⁶⁰ G. Calderini,⁶⁰ M. Carpinelli,⁶⁰ R. Cenci,⁶⁰ F. Forti,⁶⁰ M. A. Giorgi,⁶⁰ A. Lusiani,⁶⁰ G. Marchiori,⁶⁰ M. A. Mazur,⁶⁰ M. Morganti,⁶⁰ N. Neri,⁶⁰ E. Paoloni,⁶⁰ M. Rama,⁶⁰ G. Rizzo,⁶⁰ J. Walsh,⁶⁰ M. Haire,⁶¹ D. Judd,⁶¹ D. E. Wagoner,⁶¹ J. Biesiada,⁶² N. Danielson,⁶² P. Elmer,⁶² Y. P. Lau,⁶² C. Lu,⁶² J. Olsen,⁶² A. J. S. Smith,⁶² A. V. Telnov,⁶² F. Bellini,⁶³ G. Cavoto,⁶³ A. D’Orazio,⁶³ E. Di Marco,⁶³ R. Faccini,⁶³ F. Ferrarotto,⁶³ F. Ferroni,⁶³ M. Gaspero,⁶³ L. Li Gioi,⁶³ M. A. Mazzoni,⁶³ S. Morganti,⁶³ G. Piredda,⁶³ F. Polci,⁶³ F. Safai Tehrani,⁶³ C. Voena,⁶³ H. Schröder,⁶⁴ R. Waldi,⁶⁴ T. Adye,⁶⁵ N. De Groot,⁶⁵ B. Franek,⁶⁵ E. O. Olaiya,⁶⁵ F. F. Wilson,⁶⁵ S. Emery,⁶⁶ A. Gaidot,⁶⁶ S. F. Ganzhur,⁶⁶ G. Hamel de Monchenault,⁶⁶ W. Kozanecki,⁶⁶ M. Legendre,⁶⁶ B. Mayer,⁶⁶ G. Vasseur,⁶⁶ Ch. Yèche,⁶⁶ M. Zito,⁶⁶ W. Park,⁶⁷ M. V. Purohit,⁶⁷ A. W. Weidemann,⁶⁷ J. R. Wilson,⁶⁷ M. T. Allen,⁶⁸ D. Aston,⁶⁸ R. Bartoldus,⁶⁸ P. Bechtel,⁶⁸ N. Berger,⁶⁸ A. M. Boyarski,⁶⁸ R. Claus,⁶⁸ J. P. Coleman,⁶⁸ M. R. Convery,⁶⁸ M. Cristinziani,⁶⁸ J. C. Dingfelder,⁶⁸ D. Dong,⁶⁸ J. Dorfan,⁶⁸ D. Dujmic,⁶⁸ W. Dunwoodie,⁶⁸ R. C. Field,⁶⁸ T. Glanzman,⁶⁸ S. J. Gowdy,⁶⁸ V. Halyo,⁶⁸ C. Hast,⁶⁸ T. Hryn’ova,⁶⁸ W. R. Innes,⁶⁸ M. H. Kelsey,⁶⁸ P. Kim,⁶⁸ M. L. Kocian,⁶⁸ D. W. G. S. Leith,⁶⁸ J. Libby,⁶⁸ S. Luitz,⁶⁸ V. Luth,⁶⁸ H. L. Lynch,⁶⁸ D. B. MacFarlane,⁶⁸ H. Marsiske,⁶⁸ R. Messner,⁶⁸ D. R. Muller,⁶⁸ C. P. O’Grady,⁶⁸ V. E. Ozcan,⁶⁸ A. Perazzo,⁶⁸ M. Perl,⁶⁸ B. N. Ratcliff,⁶⁸ A. Roodman,⁶⁸ A. A. Salnikov,⁶⁸ R. H. Schindler,⁶⁸ J. Schwiening,⁶⁸ A. Snyder,⁶⁸ J. Stelzer,⁶⁸ D. Su,⁶⁸ M. K. Sullivan,⁶⁸ K. Suzuki,⁶⁸ S. K. Swain,⁶⁸ J. M. Thompson,⁶⁸ J. Va’vra,⁶⁸ N. van Bakel,⁶⁸ M. Weaver,⁶⁸ A. J. R. Weinstein,⁶⁸ W. J. Wisniewski,⁶⁸ M. Wittgen,⁶⁸ D. H. Wright,⁶⁸ A. K. Yarritu,⁶⁸ K. Yi,⁶⁸ C. C. Young,⁶⁸ P. R. Burchat,⁶⁹ A. J. Edwards,⁶⁹ S. A. Majewski,⁶⁹ B. A. Petersen,⁶⁹ C. Roat,⁶⁹ L. Wilden,⁶⁹ S. Ahmed,⁷⁰ M. S. Alam,⁷⁰ R. Bula,⁷⁰ J. A. Ernst,⁷⁰ V. Jain,⁷⁰ B. Pan,⁷⁰ M. A. Saeed,⁷⁰ F. R. Wappler,⁷⁰ S. B. Zain,⁷⁰ W. Bugg,⁷¹ M. Krishnamurthy,⁷¹ S. M. Spanier,⁷¹ R. Eckmann,⁷² J. L. Ritchie,⁷² A. Satpathy,⁷² R. F. Schwitters,⁷² J. M. Izen,⁷³ I. Kitayama,⁷³ X. C. Lou,⁷³ S. Ye,⁷³ F. Bianchi,⁷⁴ M. Bona,⁷⁴ F. Gallo,⁷⁴ D. Gamba,⁷⁴ M. Bomben,⁷⁵ L. Bosisio,⁷⁵ C. Cartaro,⁷⁵ F. Cossutti,⁷⁵ G. Della Ricca,⁷⁵ S. Dittongo,⁷⁵ S. Grancagnolo,⁷⁵ L. Lancieri,⁷⁵ L. Vitale,⁷⁵ V. Azzolini,⁷⁶ F. Martinez-Vidal,⁷⁶ R. S. Panvini,^{77,¶} Sw. Banerjee,⁷⁸ B. Bhuyan,⁷⁸ C. M. Brown,⁷⁸ D. Fortin,⁷⁸ K. Hamano,⁷⁸ R. Kowalewski,⁷⁸ I. M. Nugent,⁷⁸ J. M. Roney,⁷⁸ R. J. Sobie,⁷⁸ J. J. Back,⁷⁹ P. F. Harrison,⁷⁹ T. E. Latham,⁷⁹ G. B. Mohanty,⁷⁹ H. R. Band,⁸⁰ X. Chen,⁸⁰ B. Cheng,⁸⁰ S. Dasu,⁸⁰ M. Datta,⁸⁰ A. M. Eichenbaum,⁸⁰ K. T. Flood,⁸⁰ M. T. Graham,⁸⁰ J. J. Hollar,⁸⁰ J. R. Johnson,⁸⁰ P. E. Kutter,⁸⁰ H. Li,⁸⁰ R. Liu,⁸⁰ B. Mellado,⁸⁰ A. Mihalys,⁸⁰ A. K. Mohapatra,⁸⁰ Y. Pan,⁸⁰ M. Pierini,⁸⁰ R. Prepost,⁸⁰ P. Tan,⁸⁰ S. L. Wu,⁸⁰ Z. Yu,⁸⁰ and H. Neal⁸¹

(The BABAR Collaboration)

¹Laboratoire de Physique des Particules, F-74941 Annecy-le-Vieux, France

²Universitat de Barcelona, Fac. Física Dept. ECM,

Avda Diagonal 647, 6a planta, E-08028 Barcelona, Spain

³Università di Bari, Dipartimento di Fisica and INFN, I-70126 Bari, Italy

⁴Institute of High Energy Physics, Beijing 100039, China

⁵University of Bergen, Institute of Physics, N-5007 Bergen, Norway

⁶Lawrence Berkeley National Laboratory and University of California, Berkeley, California 94720, USA

⁷University of Birmingham, Birmingham, B15 2TT, United Kingdom

⁸Ruhr Universität Bochum, Institut für Experimentalphysik 1, D-44780 Bochum, Germany

⁹University of Bristol, Bristol BS8 1TL, United Kingdom

¹⁰University of British Columbia, Vancouver, British Columbia, Canada V6T 1Z1

¹¹Brunel University, Uxbridge, Middlesex UB8 3PH, United Kingdom

¹²Budker Institute of Nuclear Physics, Novosibirsk 630090, Russia

- ¹³ University of California at Irvine, Irvine, California 92697, USA
¹⁴ University of California at Los Angeles, Los Angeles, California 90024, USA
¹⁵ University of California at Riverside, Riverside, California 92521, USA
¹⁶ University of California at San Diego, La Jolla, California 92093, USA
¹⁷ University of California at Santa Barbara, Santa Barbara, California 93106, USA
¹⁸ University of California at Santa Cruz, Institute for Particle Physics, Santa Cruz, California 95064, USA
¹⁹ California Institute of Technology, Pasadena, California 91125, USA
²⁰ University of Cincinnati, Cincinnati, Ohio 45221, USA
²¹ University of Colorado, Boulder, Colorado 80309, USA
²² Colorado State University, Fort Collins, Colorado 80523, USA
²³ Universität Dortmund, Institut für Physik, D-44221 Dortmund, Germany
²⁴ Technische Universität Dresden, Institut für Kern- und Teilchenphysik, D-01062 Dresden, Germany
²⁵ Ecole Polytechnique, LLR, F-91128 Palaiseau, France
²⁶ University of Edinburgh, Edinburgh EH9 3JZ, United Kingdom
²⁷ Università di Ferrara, Dipartimento di Fisica and INFN, I-44100 Ferrara, Italy
²⁸ Laboratori Nazionali di Frascati dell'INFN, I-00044 Frascati, Italy
²⁹ Università di Genova, Dipartimento di Fisica and INFN, I-16146 Genova, Italy
³⁰ Harvard University, Cambridge, Massachusetts 02138, USA
³¹ Universität Heidelberg, Physikalisches Institut, Philosophenweg 12, D-69120 Heidelberg, Germany
³² Imperial College London, London, SW7 2AZ, United Kingdom
³³ University of Iowa, Iowa City, Iowa 52242, USA
³⁴ Iowa State University, Ames, Iowa 50011-3160, USA
³⁵ Universität Karlsruhe, Institut für Experimentelle Kernphysik, D-76021 Karlsruhe, Germany
³⁶ Laboratoire de l'Accélérateur Linéaire, IN2P3-CNRS et Université Paris-Sud 11, Centre Scientifique d'Orsay, B.P. 34, F-91898 ORSAY Cedex, France
³⁷ Lawrence Livermore National Laboratory, Livermore, California 94550, USA
³⁸ University of Liverpool, Liverpool L69 7ZE, United Kingdom
³⁹ Queen Mary, University of London, E1 4NS, United Kingdom
⁴⁰ University of London, Royal Holloway and Bedford New College, Egham, Surrey TW20 0EX, United Kingdom
⁴¹ University of Louisville, Louisville, Kentucky 40292, USA
⁴² University of Manchester, Manchester M13 9PL, United Kingdom
⁴³ University of Maryland, College Park, Maryland 20742, USA
⁴⁴ University of Massachusetts, Amherst, Massachusetts 01003, USA
⁴⁵ Massachusetts Institute of Technology, Laboratory for Nuclear Science, Cambridge, Massachusetts 02139, USA
⁴⁶ McGill University, Montréal, Québec, Canada H3A 2T8
⁴⁷ Università di Milano, Dipartimento di Fisica and INFN, I-20133 Milano, Italy
⁴⁸ University of Mississippi, University, Mississippi 38677, USA
⁴⁹ Université de Montréal, Physique des Particules, Montréal, Québec, Canada H3C 3J7
⁵⁰ Mount Holyoke College, South Hadley, Massachusetts 01075, USA
⁵¹ Università di Napoli Federico II, Dipartimento di Scienze Fisiche and INFN, I-80126, Napoli, Italy
⁵² NIKHEF, National Institute for Nuclear Physics and High Energy Physics, NL-1009 DB Amsterdam, The Netherlands
⁵³ University of Notre Dame, Notre Dame, Indiana 46556, USA
⁵⁴ Ohio State University, Columbus, Ohio 43210, USA
⁵⁵ University of Oregon, Eugene, Oregon 97403, USA
⁵⁶ Università di Padova, Dipartimento di Fisica and INFN, I-35131 Padova, Italy
⁵⁷ Universités Paris VI et VII, Laboratoire de Physique Nucléaire et de Hautes Energies, F-75252 Paris, France
⁵⁸ University of Pennsylvania, Philadelphia, Pennsylvania 19104, USA
⁵⁹ Università di Perugia, Dipartimento di Fisica and INFN, I-06100 Perugia, Italy
⁶⁰ Università di Pisa, Dipartimento di Fisica, Scuola Normale Superiore and INFN, I-56127 Pisa, Italy
⁶¹ Prairie View A&M University, Prairie View, Texas 77446, USA
⁶² Princeton University, Princeton, New Jersey 08544, USA
⁶³ Università di Roma La Sapienza, Dipartimento di Fisica and INFN, I-00185 Roma, Italy
⁶⁴ Universität Rostock, D-18051 Rostock, Germany
⁶⁵ Rutherford Appleton Laboratory, Chilton, Didcot, Oxon, OX11 0QX, United Kingdom
⁶⁶ DSM/Dapnia, CEA/Saclay, F-91191 Gif-sur-Yvette, France
⁶⁷ University of South Carolina, Columbia, South Carolina 29208, USA
⁶⁸ Stanford Linear Accelerator Center, Stanford, California 94309, USA
⁶⁹ Stanford University, Stanford, California 94305-4060, USA
⁷⁰ State University of New York, Albany, New York 12222, USA
⁷¹ University of Tennessee, Knoxville, Tennessee 37996, USA
⁷² University of Texas at Austin, Austin, Texas 78712, USA
⁷³ University of Texas at Dallas, Richardson, Texas 75083, USA
⁷⁴ Università di Torino, Dipartimento di Fisica Sperimentale and INFN, I-10125 Torino, Italy
⁷⁵ Università di Trieste, Dipartimento di Fisica and INFN, I-34127 Trieste, Italy

⁷⁶IFIC, Universitat de Valencia-CSIC, E-46071 Valencia, Spain

⁷⁷Vanderbilt University, Nashville, Tennessee 37235, USA

⁷⁸University of Victoria, Victoria, British Columbia, Canada V8W 3P6

⁷⁹Department of Physics, University of Warwick, Coventry CV4 7AL, United Kingdom

⁸⁰University of Wisconsin, Madison, Wisconsin 53706, USA

⁸¹Yale University, New Haven, Connecticut 06511, USA

(Dated: March 1, 2006)

We present updated results on time-dependent CP asymmetries in fully reconstructed $B^0 \rightarrow D^{(*)\pm} \pi^\mp$ and $B^0 \rightarrow D^\pm \rho^\mp$ decays in approximately 232 million $\Upsilon(4S) \rightarrow B\bar{B}$ events collected with the BABAR detector at the PEP-II asymmetric-energy B factory at SLAC. From a time-dependent maximum likelihood fit we obtain for the parameters related to the CP violation angle $2\beta + \gamma$:

$$\begin{aligned} a^{D\pi} &= -0.010 \pm 0.023 \pm 0.007, & c_{\text{lep}}^{D\pi} &= -0.033 \pm 0.042 \pm 0.012, \\ a^{D^*\pi} &= -0.040 \pm 0.023 \pm 0.010, & c_{\text{lep}}^{D^*\pi} &= 0.049 \pm 0.042 \pm 0.015, \\ a^{D\rho} &= -0.024 \pm 0.031 \pm 0.009, & c_{\text{lep}}^{D\rho} &= -0.098 \pm 0.055 \pm 0.018, \end{aligned}$$

where the first error is statistical and the second is systematic. Using other measurements and theoretical assumptions, we interpret the results in terms of the angles of the Cabibbo-Kobayashi-Maskawa unitarity triangle and find $|\sin(2\beta + \gamma)| > 0.64$ (0.40) at 68% (90%) confidence level.

PACS numbers: 12.15.Hh, 11.30.Er, 13.25.Hw

In the Standard Model, CP violation in the weak interactions between quarks manifests itself as a non-zero area of the Cabibbo-Kobayashi-Maskawa (CKM) unitarity triangle [1]. While the measurement of $\sin 2\beta$ is now quite precise [2, 3], the constraints on the other two angles of the unitarity triangle, α and γ , are still limited by statistical and theoretical uncertainties.

This paper presents updates for the measurements of CP asymmetries in $B^0 \rightarrow D^{(*)\pm} \pi^\mp$ decays [4], as reported in Ref. [5], with a larger data sample ($\times 2.6$), and in addition includes the measurement of the CP asymmetry in the decay mode $B^0 \rightarrow D^\pm \rho^\mp$. We denote these decays as $B^0 \rightarrow D^{(*)\pm} h^\mp$, where h^\mp is a charged pion or ρ meson.

The time evolution of $B^0 \rightarrow D^{(*)\pm} h^\mp$ decays is sensitive to γ because the CKM-favored decay amplitude $\bar{B}^0 \rightarrow D^{(*)+} h^-$, which is proportional to the CKM matrix elements $V_{cb} V_{ud}^*$, and the doubly-CKM-suppressed decay amplitude $B^0 \rightarrow D^{(*)+} h^-$, which is proportional to $V_{cd} V_{ub}^*$, interfere due to $B^0 - \bar{B}^0$ mixing. The relative weak phase between these two amplitudes is γ . With $B^0 - \bar{B}^0$ mixing, the total weak phase difference between the interfering amplitudes is $2\beta + \gamma$.

Neglecting the very small decay width difference between the two B^0 mass eigenstates [6], the proper-time distribution of the $B^0 \rightarrow D^{(*)\pm} h^\mp$ decays is given by

$$f^\pm(\eta, \Delta t) = \frac{e^{-|\Delta t|/\tau}}{4\tau} \times [1 \mp S_\zeta \sin(\Delta m_d \Delta t) \mp \eta C \cos(\Delta m_d \Delta t)], \quad (1)$$

where τ is the B^0 lifetime, Δm_d is the $B^0 - \bar{B}^0$ mixing frequency, and $\Delta t = t_{\text{rec}} - t_{\text{tag}}$ is the time difference between the $B^0 \rightarrow D^{(*)\pm} h^\mp$ decay (B_{rec}) and the decay of the other B (B_{tag}) from the $\Upsilon(4S) \rightarrow B^0 \bar{B}^0$ decay. In this equation the upper (lower) sign refers to the flavor of B_{tag}

as B^0 (\bar{B}^0), while $\eta = +1$ (-1) and $\zeta = +$ ($-$) for the final state $D^{(*)-} h^+$ ($D^{(*)+} h^-$). The sine term is due to interference between direct decay and decay after $B^0 - \bar{B}^0$ mixing. The cosine term arises from interference between decay amplitudes with different weak and strong phases (direct CP violation) or from CP violation in mixing. The S and C asymmetry parameters can be expressed as

$$S_\pm = -\frac{2\text{Im}(\lambda_\pm)}{1 + |\lambda_\pm|^2}, \quad \text{and} \quad C = \frac{1 - r^2}{1 + r^2}, \quad (2)$$

where $r \equiv |\lambda_+| = 1/|\lambda_-|$ and

$$\lambda_\pm = \frac{q A(\bar{B}^0 \rightarrow D^{(*)\mp} h^\pm)}{p A(B^0 \rightarrow D^{(*)\mp} h^\pm)} = r^{\pm 1} e^{-i(2\beta + \gamma \mp \delta)}. \quad (3)$$

Here $\frac{q}{p}$ is a function of the elements of the mixing Hamiltonian [6], and δ is the relative strong phase between the two contributing amplitudes. In the Standard Model, CP violation in mixing is negligible and thus $|\frac{q}{p}| = 1$. In these equations, the parameters r and δ depend on the choice of the final state. They will be indicated as $r^{D\pi}$, $\delta^{D\pi}$ for the $B^0 \rightarrow D^\pm \pi^\mp$ mode, $r^{D\rho}$, $\delta^{D\rho}$ for $B^0 \rightarrow D^\pm \rho^\mp$, and $r^{D^*\pi}$, $\delta^{D^*\pi}$ for $B^0 \rightarrow D^{*\pm} \pi^\mp$ [7, 8].

Interpreting the S parameters in terms of the angles of the unitarity triangle requires knowledge of the corresponding r parameters. The values of r are expected to be small (~ 0.02) and therefore cannot be extracted from the measurement of C . They can be estimated, assuming $SU(3)$ symmetry and neglecting contributions from W -exchange diagrams, from the ratios of branching fractions $\mathcal{B}(B^0 \rightarrow D_s^{(*)+} \pi^-) / \mathcal{B}(B^0 \rightarrow D^{(*)-} \pi^+)$ and $\mathcal{B}(B^0 \rightarrow D_s^+ \rho^-) / \mathcal{B}(B^0 \rightarrow D^- \rho^+)$ [5, 9–11].

This measurement is based on 232 million $\Upsilon(4S) \rightarrow B\bar{B}$ decays, collected with the BABAR detector [12] at the

PEP-II asymmetric-energy B factory at SLAC. We use a Monte Carlo simulation of the $BABAR$ detector based on GEANT4 [13] to validate the analysis procedure and to estimate some of the backgrounds.

The event selection criteria are unchanged from our previous publication [5], except for the application of a kaon veto on the pion candidate in the decay modes $D^{(*)-}\pi^+$ to suppress $B^0 \rightarrow D^{(*)-}K^+$ background events, and for the addition of the decay mode $B^0 \rightarrow D^-\rho^+$. The D^{*-} is reconstructed through its decay to $\bar{D}^0\pi^-$, where the \bar{D}^0 decays into $K^+\pi^-$, $K^+\pi^-\pi^0$, $K^+\pi^-\pi^+\pi^-$, or $K_s^0\pi^+\pi^-$. The D^- is reconstructed through its decay into $K^+\pi^-\pi^-$ or $K_s^0\pi^-$. The ρ^+ decay is reconstructed in the final state $\pi^+\pi^0$. For the CP analysis we require the $\pi^+\pi^0$ invariant mass ($m_{\pi\pi^0}$) to be in the window $620 < m_{\pi\pi^0} < 920$ MeV/ c^2 . Exploiting the polarization of the ρ meson from the decay $B^0 \rightarrow D^-\rho^+$ we require the cosine of the ρ^+ helicity angle θ_{hel} , defined as the angle between the charged pion and the D^- momentum in the ρ^+ rest frame, to satisfy $|\cos\theta_{\text{hel}}| > 0.4$.

The beam-energy substituted mass, $m_{\text{ES}} \equiv \sqrt{s/4 - p_B^{*2}}$, and the difference between the B candidate's measured energy and the beam energy, $\Delta E \equiv E_B^* - (\sqrt{s}/2)$, are used to identify the final sample, where E_B^* (p_B^*) is the energy (momentum) of the B candidate in the nominal e^+e^- center-of-mass frame, and \sqrt{s} is the total center-of-mass energy. The ΔE signal region is defined as $|\Delta E| < 3\sigma$, where the resolution σ is mode-dependent and approximately 20 MeV, as determined from data. Figure 1 shows the m_{ES} distribution for candidates with $m_{\text{ES}} > 5.2$ GeV/ c^2 in the ΔE signal region. These candidates satisfy the tagging and vertexing requirements, which are described later. Each distribution is fit to the sum of a threshold function [14], which accounts for the background from random combinations of tracks (combinatorial background), and a Gaussian distribution with a fitted width of about 2.5 MeV/ c^2 , which describes the signal and the backgrounds that peak in the m_{ES} signal region (peaking background). Signal yields and sample purities are determined in the m_{ES} signal region, with $m_{\text{ES}} > 5.27$ GeV/ c^2 , and are summarized in Table I. Backgrounds from B^0 and B^+ decays that peak in the m_{ES} signal region are estimated using Monte Carlo events and are mostly due to charmed final states. They are also reported in Table I.

For the $B^0 \rightarrow D^\pm\rho^\mp$ mode we consider additional sources of background with the same final state $D^\pm\pi^\mp\pi^0$, where the $\pi^\mp\pi^0$ system is not produced through the ρ^\mp resonance. Interfering sources of background can introduce a dependence of the $\lambda_{\pm}^{D\rho}$ parameters of Eq. 3 on $m_{\pi\pi^0}$. The dependency has been studied using the distribution of $m_{\pi\pi^0}$.

The possible background contributions have been evaluated with a sample of 130273 $B^0 \rightarrow D^-\pi^+\pi^0$ candidates,

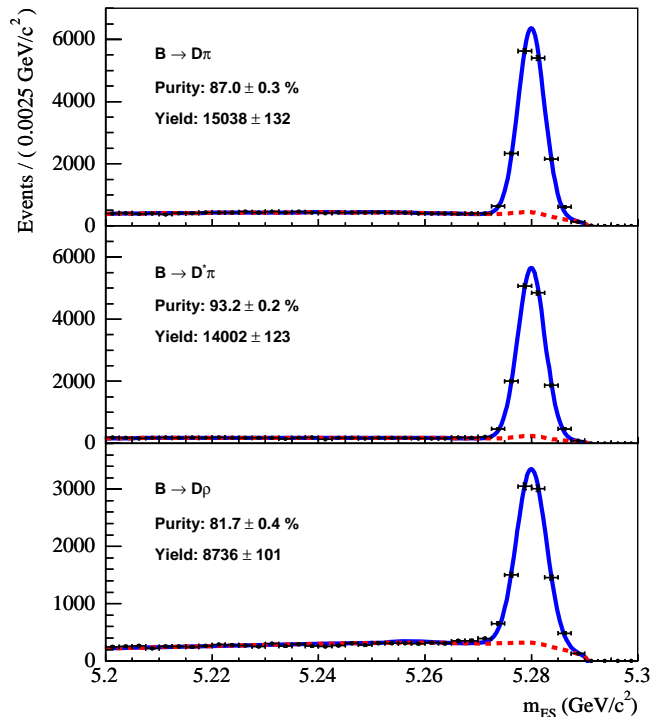


FIG. 1: m_{ES} distributions in the signal region for, from top to bottom, the $B \rightarrow D^\pm\pi^\mp$, $B \rightarrow D^{*\pm}\pi^\mp$, and $B \rightarrow D^\pm\rho^\mp$ sample for the events that satisfy the tagging and vertexing requirements described in the text, fit with the function described in the text. The dashed lines indicate the sum of the combinatorial and peaking background contributions.

TABLE I: Signal yields, sample purities P , and fractions of peaking backgrounds, f_{peak} , for the selected samples for events that satisfy the tagging and vertexing requirements described in the text.

Decay mode	Yield	$P(\%)$	$f_{\text{peak}}(\%)$	
			B^0	B^\pm
$B \rightarrow D^\pm\pi^\mp$	15038 ± 132	87.0 ± 0.3	1.6 ± 0.1	1.2 ± 0.1
$B \rightarrow D^{*\pm}\pi^\mp$	14002 ± 123	93.2 ± 0.2	1.0 ± 0.1	1.1 ± 0.1
$B \rightarrow D^\pm\rho^\mp$	8736 ± 101	81.7 ± 0.4	1.3 ± 0.2	1.5 ± 0.2

on which the requirements on the ρ helicity and on $m_{\pi\pi^0}$ have been removed. Three interfering components are considered: $B^0 \rightarrow D^-\rho^+$ (the signal), $B^0 \rightarrow D^-\rho'^+(1450)$ with a pole mass of (1465 ± 25) MeV/ c^2 and a width of (400 ± 60) MeV/ c^2 [6] for the ρ'^+ , both described with P-wave relativistic Breit-Wigner functions [15, 16], and a non-resonant component, $B^0 \rightarrow D^-(\pi^+\pi^0)_{nr}$. Contributions from the decay modes $B^0 \rightarrow D^{*-}\pi^+$ ($D^{*-} \rightarrow D^-\pi^0$) and $B^0 \rightarrow \bar{D}^{*0}\pi^0$ ($\bar{D}^{*0} \rightarrow D^-\pi^+$) are negligible due to the kinematic constraints imposed on the ρ daughter particles. We perform a fit to the binned $m_{\pi\pi^0}$ distribution to extract the amplitudes of the three components, where for each bin the combinatorial background has been subtracted, as estimated from the corresponding m_{ES} dis-

tribution, and the number of peaking background events has been estimated using fully simulated Monte Carlo events. The result of the fit is shown in Fig. 2. The fraction of $B^0 \rightarrow D^- \rho'^+$ (1450) and $B^0 \rightarrow D^- (\pi^+ \pi^0)_{nr}$ events in the mass window $620 < m_{\pi\pi^0} < 920$ MeV/c² is found to be smaller than 0.02 at 90% confidence level (C.L.)

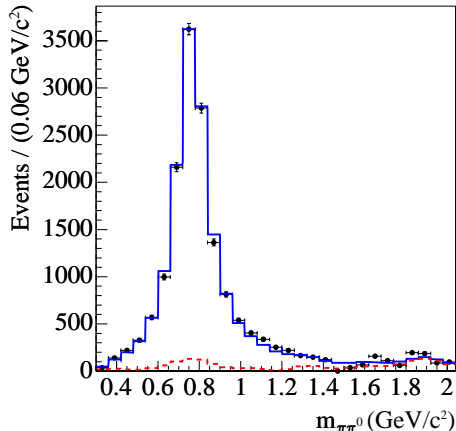


FIG. 2: $m_{\pi\pi^0}$ distribution for the combinatorial-background subtracted $B \rightarrow D^\pm \pi^\mp \pi^0$ sample, containing 16214 events. The solid line is the fit projection, consisting of the three interfering components described in the text and an m_{ES} peaking background contribution, indicated with the dashed line.

The proper time interval Δt between the two B decays is calculated from the measured separation Δz , between the B_{rec} and B_{tag} decay points along the beam direction. We determine the B_{rec} decay point from its charged tracks. The B_{tag} decay point is obtained by fitting tracks that do not belong to B_{rec} , imposing constraints from the B_{rec} momentum and the beam-spot location. We accept events with calculated Δt uncertainty of less than 2.5 ps and $|\Delta t| < 20$ ps. The average Δt resolution is approximately 1.1 ps. We use multivariate algorithms that identify signatures in the B_{tag} decay products to determine (“tag”) the flavor to be either a B^0 or a \bar{B}^0 [2]. Primary leptons from semileptonic B decays are selected from identified electrons and muons and from isolated energetic tracks. The charges of identified kaons and soft pions from D^{*+} decays are also used to extract flavor information. Each event with an estimated mistag probability less than 45% is assigned to one of six hierarchical, mutually exclusive tagging categories. The lepton tagging category contains events with an identified lepton, while other events are divided into categories based on their estimated mistag probability. The effective efficiency of the tagging algorithm, defined as $Q = \sum_i \epsilon_i (1 - 2w_i)^2$, where ϵ_i and w_i are the efficiency and the mistag probability, respectively, for category i , is $30.1 \pm 0.5\%$.

Since the expected CP asymmetry in the selected B decays is small, this measurement is sensitive to the in-

terference between the $b \rightarrow u$ and $b \rightarrow c$ amplitudes in the decay of B_{tag} . To account for this “tagside interference”, we use a parametrization different from Eq. 2, which is described in Ref. [17] and summarized here. For each tagging category i , independent of the decay mode $\mu \in \{D\pi, D^*\pi, D\rho\}$, the tagside interference is parametrized in terms of the effective parameters r'_i and δ'_i . Neglecting terms of order $(r^\mu)^2$ and $(r'_i)^2$, the Δt distributions are written as

$$f_i^{\pm;\mu}(\eta, \Delta t) = \frac{e^{-|\Delta t|/\tau}}{4\tau} \times [1 \mp (a^\mu \mp \eta b_i - \eta c_i^\mu) \sin(\Delta m_d \Delta t) \mp \eta \cos(\Delta m_d \Delta t)], \quad (4)$$

where, in the Standard Model,

$$\begin{aligned} a^\mu &= 2r^\mu \sin(2\beta + \gamma) \cos \delta^\mu, \\ b_i &= 2r'_i \sin(2\beta + \gamma) \cos \delta'_i, \\ c_i^\mu &= 2 \cos(2\beta + \gamma) (r^\mu \sin \delta^\mu - r'_i \sin \delta'_i). \end{aligned} \quad (5)$$

Semileptonic B decays do not have a doubly-CKM-suppressed amplitude contribution, and hence $r'_{lep} = 0$. In the following, we quote results for the six a^μ and c_{lep}^μ parameters, which are independent of the unknown parameters r'_i and δ'_i . The other b_i and c_i^μ parameters depend on r'_i and δ'_i , and do not contribute to the interpretation of the result in terms of $\sin(2\beta + \gamma)$. Note that all tagging categories contribute to the measurement of the a^μ parameters.

An unbinned maximum-likelihood fit is applied to the Δt distribution of the selected B candidates in the ΔE signal region. The whole m_{ES} range is used to determine the signal probability of each event on the basis of the Argus plus Gaussian fit described previously. The effect of finite Δt resolution is described by convoluting Eq. 4 with a resolution function composed of three Gaussian distributions. Incorrect tagging dilutes the parameters a^μ , c_i^μ , and the coefficient of $\cos(\Delta m_d \Delta t)$ by a factor $D_i = 1 - 2w_i$ [2]. The parameters of the resolution function and those associated with flavor tagging are determined from the fit to the data and are consistent with previous BABAR analyses [2]. The Δt distribution of the combinatorial background is parametrized using two empirical components: a prompt component with zero lifetime and a component with an effective lifetime. The components are convoluted with the sum of two Gaussians, and the resolution parameters of the two Gaussians, including the effective dilution parameters, the effective lifetime, and the relative fraction of the two components, are determined from the fit to the data. The peaking background coming from B^\pm mesons is modeled by an exponential with the B^\pm lifetime. Its relative fraction is fixed to the value estimated from simulations. The resolution function is the same as the signal resolution, while the dilution parameters are fixed to the values obtained from a B^+ control sample. The peaking backgrounds from B^0 mesons, whose amounts are also fixed to

the value estimated using simulation, are modeled with a likelihood similar to the signal likelihood, but without CP violation (all the a , b , c parameters set to zero). Possible CP violation in this background is taken into account in the evaluation of the systematic uncertainties. The resolution and the dilution parameters are the same as for the signal.

From the unbinned maximum likelihood fit we obtain:

$$\begin{aligned}
a^{D\pi} &= -0.010 \pm 0.023 \pm 0.007, & (6) \\
c_{\text{lep}}^{D\pi} &= -0.033 \pm 0.042 \pm 0.012, \\
a^{D^*\pi} &= -0.040 \pm 0.023 \pm 0.010, \\
c_{\text{lep}}^{D^*\pi} &= 0.049 \pm 0.042 \pm 0.015, \\
a^{D\rho} &= -0.024 \pm 0.031 \pm 0.009, \\
c_{\text{lep}}^{D\rho} &= -0.098 \pm 0.055 \pm 0.018,
\end{aligned}$$

where the first quoted error is statistical and the second is systematic. The largest correlation with any linear combination of other fit parameters is about 20% and 30% for the a^μ and the c_{lep}^μ parameters, respectively. Figure 3 shows the fitted Δt distributions for events from the lepton tagging category, which has the lowest level of background and mistag probability. The various contributions to the systematic uncertainties of the a and c_{lep} parameters are shown in Table II.

TABLE II: Systematic uncertainties on the a and c_{lep} parameters (in units of 10^{-2}).

B^0 mode	$D^\pm\pi^\mp$		$D^{*\pm}\pi^\mp$		$D^\pm\rho^\mp$	
Source	σ_a	σ_c	σ_a	σ_c	σ_a	σ_c
Vertexing ($\sigma_{\Delta t}$)	0.37	0.64	0.80	1.14	0.47	1.15
Fit (σ_{fit})	0.51	0.95	0.52	0.99	0.75	1.34
Model (σ_{mod})	0.12	0.13	0.12	0.13	0.01	0.18
Tagging (σ_{tag})	0.07	0.16	0.11	0.14	0.06	0.12
Background (σ_{bkg})	0.13	0.10	0.10	0.09	0.28	0.29
$m_{\pi\pi^0}$ Dependence (σ_λ)	—	—	—	—	0.16	0.16
Total (σ_{tot})	0.66	1.17	0.97	1.53	0.94	1.81

The impact of a possible systematic mismeasurement of Δt ($\sigma_{\Delta t}$) has been estimated by comparing different parameterizations of the resolution function, varying the position of the beam spot and the absolute z scale within their uncertainties, and loosening and tightening the quality criteria on the reconstructed decay points. We also estimate the impact of the uncertainties on the alignment of the silicon vertex tracker (SVT) by repeating the measurement using simulated events, with the SVT intentionally misaligned. For the systematic uncertainty of the fit (σ_{fit}), we quote the upper limit on the bias on the a^μ and c^μ parameters, as estimated from samples of fully-simulated events. The model error (σ_{mod}) contains the uncertainty on the B^0 lifetime and Δm_d , varied by the uncertainties on the world averages [6] and also by allowing them to vary in the fit. The tagging error (σ_{tag})

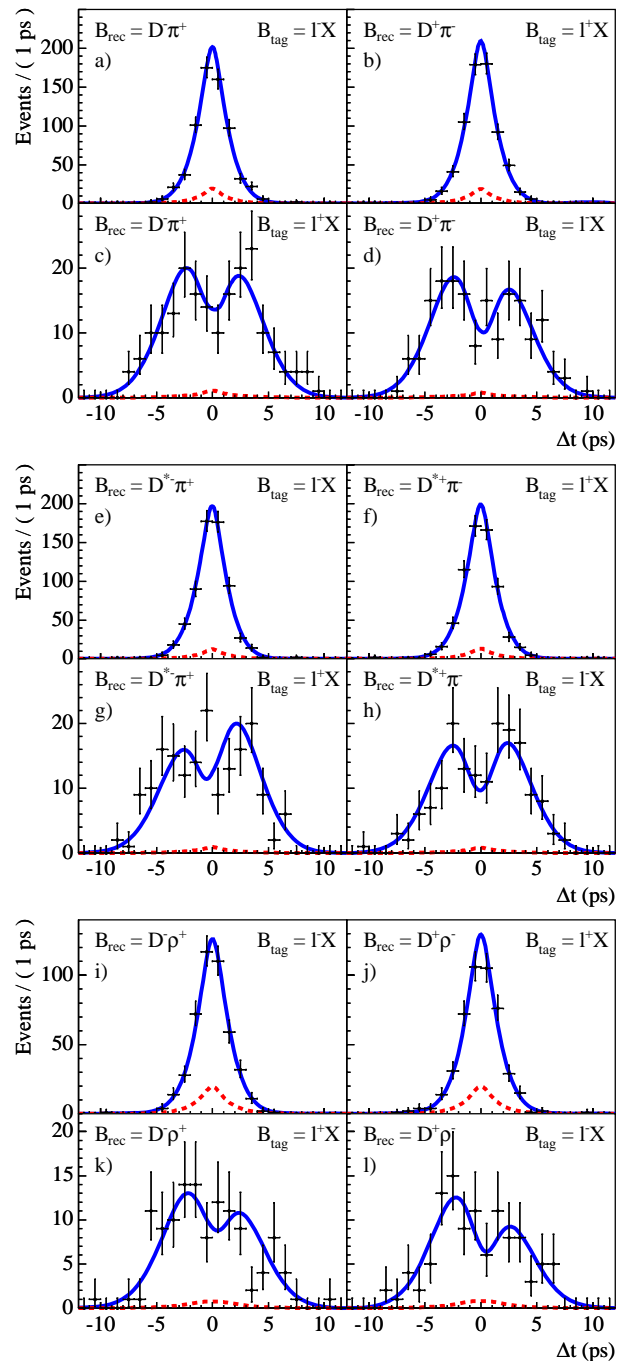


FIG. 3: Distributions of Δt for the $B^0 \rightarrow D^\pm\pi^\mp$ (a-d), $B^0 \rightarrow D^{*\pm}\pi^\mp$ (e-h), and $B^0 \rightarrow D^\pm\rho^\mp$ (i-l) candidates tagged with leptons, split by B tagging flavor and reconstructed final state. The solid lines are fit projections. The background contributions are represented by the dashed curves.

is estimated considering possible differences in tagging efficiency between B^0 and \bar{B}^0 , different mistag fractions for the decay modes $D\pi$, $D^*\pi$, $D\rho$, and different Δt resolutions for correctly and incorrectly tagged events. We also account for uncertainties in the background (σ_{bkg})

by varying the effective lifetimes, dilutions, m_{ES} shape parameters, signal fractions, and background CP asymmetry. A possible dependence of $a^{D\rho}$ ($c_{lep}^{D\rho}$) on the $\pi\pi^0$ invariant mass (σ_λ) is estimated from the limit on the fraction of $B^0 \rightarrow D^- \rho'^+(1450)$ and $B^0 \rightarrow D^- (\pi^+ \pi^0)_{nr}$ in the ρ mass window.

As a cross-check, we perform the same fits on a sample of 6843 $B^- \rightarrow D^{(*)0} \pi^-$ candidates, where, as expected, we find no CP asymmetries. We combine our results with the result obtained on the partially reconstructed $B \rightarrow D^{*\pm} \pi^\mp$ sample [10] and use a frequentist method described in Ref. [10] to set a constraint on $2\beta + \gamma$. The confidence level as a function of $|\sin(2\beta + \gamma)|$ is shown in Figure 4. We set the lower limits $|\sin(2\beta + \gamma)| > 0.64$ (0.40) at 68% (90%) C.L.

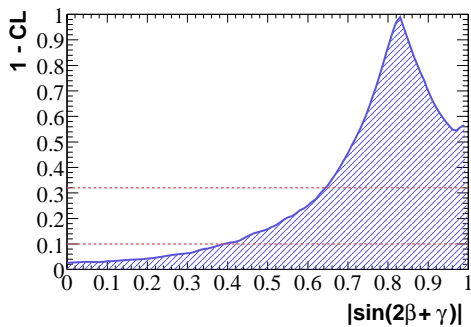


FIG. 4: Frequentist confidence level as a function of $|\sin(2\beta + \gamma)|$, obtained when combining our result with the result obtained on partially reconstructed $B \rightarrow D^{*\pm} \pi^\mp$ decays [10]. The horizontal lines show the 68% (top) and 90% C.L. (bottom).

In conclusion, we have studied the time-dependent CP -violating asymmetries in fully reconstructed $B^0 \rightarrow D^\pm \pi^\mp$, $B^0 \rightarrow D^{*\pm} \pi^\mp$, and $B^0 \rightarrow D^\pm \rho^\mp$ decays in a sample of 232 million $\Upsilon(4S) \rightarrow B\bar{B}$ decays, and have measured the CP -violating parameters listed in Eq. 6. We interpret the result in terms of $\sin(2\beta + \gamma)$ and find that $|\sin(2\beta + \gamma)| > 0.64$ (0.40) at 68% (90%) C.L. These results are consistent with and supersede our previous measurement.

We are grateful for the excellent luminosity and machine conditions provided by our PEP-II colleagues, and for the substantial dedicated effort from the computing organizations that support BABAR. The collaborating institutions wish to thank SLAC for its support and kind hospitality. This work is supported by DOE and NSF (USA), NSERC (Canada), IHEP (China), CEA and CNRS-IN2P3 (France), BMBF and DFG (Germany), INFN (Italy), FOM (The Netherlands), NFR (Norway),

MIST (Russia), and PPARC (United Kingdom). Individuals have received support from CONACyT (Mexico), Marie Curie EIF (European Union), the A. P. Sloan Foundation, the Research Corporation, and the Alexander von Humboldt Foundation.

* Also with the Johns Hopkins University, Baltimore, Maryland 21218, USA

† Also at Laboratoire de Physique Corpusculaire, Clermont-Ferrand, France

‡ Also with Università di Perugia, Dipartimento di Fisica, Perugia, Italy

§ Also with Università della Basilicata, Potenza, Italy

¶ Deceased

- [1] N. Cabibbo, Phys. Rev. Lett. **10**, 531 (1963); M. Kobayashi and T. Maskawa, Prog. Theor. Phys. **49**, 652 (1973).
- [2] BABAR Collaboration, B. Aubert *et al.*, Phys. Rev. Lett. **94**, 161803 (2005).
- [3] Belle Collaboration, K. Abe *et al.*, Phys. Rev. D **71**, 072003 (2005).
- [4] Charge conjugation is implied in this paper, unless otherwise stated. The superscript (*) indicates that the superscripted symbol must be considered both with and without the *.
- [5] BABAR Collaboration, B. Aubert *et al.*, Phys. Rev. Lett. **92**, 251801 (2004).
- [6] Particle Data Group, S. Eidelman *et al.*, Phys. Lett. B **592**, 1 (2004).
- [7] R. Fleischer, Nucl. Phys. B **671**, 459 (2003).
- [8] According to Ref. [7], the strong phase difference for $B^0 \rightarrow D^{*\pm} \pi^\mp$ is given by $\delta^{D^*} \pi + \pi$, but this does not affect this measurement.
- [9] I. Dunietz, Phys. Lett. B **427**, 179 (1998); I. Dunietz and R.G. Sachs, Phys. Rev. D **37**, 3186 (1988).
- [10] BABAR Collaboration, B. Aubert *et al.*, Phys. Rev. D **71**, 112003 (2005).
- [11] BABAR Collaboration, B. Aubert *et al.*, SLAC-PUB-10602, hep-ex/0408029, submitted to the 32nd International Conference on High-Energy Physics, ICHEP 04, 16 August—22 August 2004, Beijing, China.
- [12] BABAR Collaboration, B. Aubert *et al.*, Nucl. Instr. Methods Phys. Res., Sect. C **A479**, 1 (2002).
- [13] GEANT4 Collaboration, S. Agostinelli *et al.*, Nucl. Instr. Methods Phys. Res., Sect. C **A506**, 250 (2003).
- [14] ARGUS Collaboration, H. Albrecht *et al.*, Z. Phys. **C48**, 543 (1990).
- [15] J.H. Kühn and A. Santamaria, Z. Phys. **C48**, 445 (1990).
- [16] J. Blatt and V. Weisskopf, “Theoretical Nuclear Physics”, John Wiley & Sons, New York, pag. 362, 1956.
- [17] O. Long, M. Baak, R. N. Cahn, D. Kirkby, Phys. Rev. D **68**, 034010 (2003).